

Change Detection and Classification using Hyperspectral Imagery

Indira Bidari
School of Computer Science and Engineering
KLE Technological University
Hubballi, India
indira_bidari@kletech.ac.in

Anish Mahajan
School of Computer Science and Engineering
KLE Technological University
Hubballi, India
anishmahajan809@gmail.com

Satyadhyan Chickerur
Centre for High Performance Computing, School of Computer Science and Engineering
KLE Technological University
Hubballi, India
chickerursr@kletech.ac.in

Amogh Nikkam
School of Computer Science and Engineering
KLE Technological University
Hubballi, India
amoghnikkam@gmail.com

Akshay Kulkarni
School of Computer Science and Engineering
KLE Technological University
Hubballi, India
akshaykulkarni1303@gmail.com

Sumanth Akella
School of Computer Science and Engineering
KLE Technological University
Hubballi, India
sumanth.akella2000@gmail.com

Abstract— Hyperspectral Imagery is a field with various applications in the present world. Classification and Change Detection (CD) have been fields of great importance over the years. Powerful tools are built by combining these two approaches, HSI with classification and with change detection. Deep learning-based land-cover classification and change detection algorithms have made significant advancements during recent times. In this paper, a band-specific feature extraction and classification method using 2D and 3D CNN (Hybrid Spectral Net) is being projected, which is computationally more accessible. Also, a change detection algorithm uses the Slow Feature Analysis (SFA) technique and fully connected layers of a neural network to give a binary classification. So initially, we aimed to do the multiclass classification by combining classification and change detection in one module. But a dataset with the ground truth value and bi-temporal was required, which was not available, so both classification and change detection have been implemented on different datasets.

Keywords— *Change Detection, Classification, Hyperspectral Images, Deep Learning, Hybrid Spectral Net, Slow Feature Analysis.*

I. INTRODUCTION

Hyperspectral images contain affluence of spatial information. It has abundant information as compared to a standard RGB image. The light that falls on the object's surface is reflected in many wavelengths, while our eyes can capture only the principal colors. Hyperspectral images capture many different spectral bands that include a high volume of information. In a hyperspectral image, each pixel contains spectral and spatial information, which forms the three dimensions, one of spectral as z and two of spatial as (x, y) , to create a 3-Dimensional Hyperspectral cube.

In remote sensing, Classification and Change Detection are of utmost importance because of their impact on human life. The Hyperspectral images reveal crucial information about the area of interest because of the uniqueness and abundance of spectral data. Change Detection assistances in identifying the land-use changes over a period of time. Change Detection and Classification has diverse applications in the field of monitoring landmasses. Potential applications are deforestation monitoring, border security, agricultural

variation analysis, damage assessment of buildings in urban areas..

There are various hyperspectral sensors mounted on two platforms: airborne; an example is Hyperspectral Digital Imagery Collection Experiment (HYDICE), and spaceborne; an example is Hyperion. These provide high spectral and spatial data for different applications. For change detection, the need of the data is such that the hyperspectral image taken of a specific location on a particular date and time is one input & the other input is of the same location but on a different date and time. It means we need two hyperspectral images with a difference in date and time of the exact location to identify the changes that have taken place in that duration.

II. LITERATURE SURVEY

The article [1] has distinguished change detection methods into seven groups on multi-temporal remote sensing data. The paper has also discussed the pre-processing and correction techniques. All methods have been categorized as either exterior or interior checks.

Taking the benefits of the 3D Fully Convolutional Network (FCN) and Convolutional Long Short-Term Memory (ConvLSTM), the authors in [2] have proposed a new three-dimensional Fully Convolutional Network (Re3FCN). In the generation of input data samples, they used Spectral Correlation Angle (SCA) and Principal Component Analysis (PCA). The proposed method is used for the detection of binary and multiple changes. The results of this method outperformed other methods.

In [3], Kwan has summarized different change detection methods on multi and hyperspectral images for various applications. He has mentioned multiple categories and algorithms of change detection. The author explained the possible techniques that can be used as supervised and unsupervised change detection. At last, also mentioned the challenges from the practitioner viewpoint.

The author in [4] presents a comprehensive review and analysis of change detection methods with deep learning. A graphical representation of the recent publications of change detection with deep learning models has been presented. The author has also mentioned fully supervised, fully

unsupervised, and transfer learning-based methods for change detection.

In [5], the authors have proposed a new change detection algorithm named Deep Slow Feature Analysis (DSFA), a combination of deep network and slow feature analysis. This method distinguished the change with the unchanged components. Further change vector analysis and chi-square distance have been used for change detection.

The author in [6] highlighted the classification-based approach and proposed a Hybrid Spectral CNN (HybridSN) for hyperspectral imagery. This method is a combination of spectral-spatial 3-D CNN and spatial 2-D CNN. The model was implemented with three different remote sensing datasets to analyze the performance and obtain satisfactory performance. In [7], the author combines binary and multiclass change detection on hyperspectral images using Stacked Auto-Encoders based on pixel-wise distance calculation. And for spatial information extraction used watershed segmentation. This method extracted more relevant features compared to other FE-based methods.

In the paper [8], an end-to-end approach is implemented based on a Convolutional Neural Network. This approach extracts spectral and spatial features and performs classification on Hyperspectral imagery. The paper [9] is a broad summary of the current state-of-the-art of hyperspectral imagery. The author speaks of various challenges and works in different application domains, such as classification and change detection. They mentioned three benchmark hyperspectral datasets and challenges in methods of dimensionality reduction, classification, change detection, resolution enhancement, and fast computing.

The authors in [10] have experimented with PCA, PCA with K-means, MAD, and IRMAD change detection methods on CPU and GPU platforms, and from results, it showed that PCA with k-means performed better when compared to the one listed. The dataset was of multispectral imagery. In [11], the authors have mentioned various change detection methods for HSI with experimental results. They have distinguished the algorithms into five main groups and discussed which would be appropriate for particular data. Pre-processing steps are mentioned taking various scenarios into consideration.

III. CLASSIFICATION- HYBRID SPECTRAL NET MODEL

Hybrid Spectral Net uses a combination of 2D and 3D convolution neural networks. From the spectral bands, the 3D-CNN expedites joint spatial-spectral representation. To acquire more abstract spatial representation on top of 3D-CNN 2D-CNN is used. PCA is used to reduce the number of bands. After reducing the data, we represent it as obtained after PCA is applied on it, M and N denote width and height, and spectral bands number is denoted by B . The 2D CNN processes spatial information but is not capable of processing spectral information. The 3D CNN can process both but at the cost of computational complexity. Hence both are used to achieve greater levels of accuracy. The hyperspectral cube is divided into 3D patches for better utilization of the model. These patches extract the spectral feature by providing the input HSI image to the 3D-CNN model. Then the image patch is resized and given as input to the 2D CNN. The 2D CNN works with the spatial feature maps, and then the image patch is flattened. The flattened image is given as input to the three fully connected layers, with the last layer being the SoftMax

layer. In this layer, the number of nodes will be the number of classes.

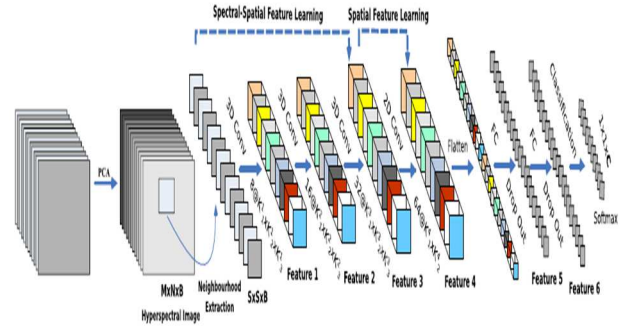


Fig. 1. Architecture of Hybrid Spectral Net

The 2D kernels are convolved with input data in a 2D-CNN. By computing the sum of dot product amongst input data and kernel the convolution is accomplished. To cover the full spatial dimension the kernel is strided. Then an activation function is adapted for the convolved features.

The 3D kernels are convolved with 3D data for the 3D convolution. To capture the spectral information and to generate the feature maps a 3D kernel is used over input layer's multiple contiguous bands.

To use classification techniques on HSI, the data cube has to be divided into 3D patches, overlapping with one another. 3D-neighbouring patches are created at spatial location (α, β) , which covers window $S \times S$ along with spectral bands (B). The width covered by the 3D patch is from $\alpha - (S - 1) / 2$ to $\alpha + (S - 1) / 2$ and the height from $\beta - (S - 1) / 2$ to $\beta + (S - 1) / 2$ and a reduced data cube from all B spectral bands after PCA.

The activation value at (x, y) spatial position in the j^{th} feature map of an i^{th} layer in the 2D convolution is denoted as $v_{i,j}^{x,y}$, which the equation below can generate:

$$v_{i,j}^{x,y} = \phi \left(b_{i,j} + \sum_{\tau=1}^{dl-1} \sum_{\rho=-\gamma}^{\gamma} \sum_{\sigma=-\delta}^{\delta} w_{i,j,\pi}^{\sigma,\rho} \times v_{i-1,\tau}^{x+\sigma,y+\rho} \right) \quad (1)$$

where the activation function is denoted as ϕ , the $b_{i,j}$ is the bias parameter for the j^{th} feature map of i^{th} layer, $dl - 1$ denotes the number of feature map in $(l - 1)^{\text{th}}$ layer and $w_{i,j}$ is the depth of the kernel, the width is given by $2\gamma + 1$ and height of the kernel is given by $2\delta + 1$ respectively whereas $w_{i,j}$ denotes the value of weight parameter.

The activation value at (x, y, z) spatial position in the j^{th} feature map of i^{th} layer in the 3D convolution is denoted as $v_{i,j}^{x,y,z}$, which can be generated by the equation :

$$v_{i,j}^{x,y,z} = \theta \left(b_{i,j} + \sum_{\tau=1}^{dl-1} \sum_{\lambda=-\eta}^{\eta} \sum_{\rho=-\gamma}^{\gamma} \sum_{\sigma=-\delta}^{\delta} w_{i,j,\pi}^{\sigma,\rho,\lambda} \times v_{i-1,\tau}^{x+\sigma,y+\rho,z+\lambda} \right) \quad (2)$$

where the kernel depth along spectral dimension is $2\eta + 1$ and remaining parameters are similar as in 2D convolution.

Supervised approach is used to train b as bias and w as the kernel weight parameters along with gradient descent optimization technique.

IV. CHANGE DETECTION- DEEP SLOW FEATURE ANALYSIS (DSFA)

The deep slow feature analysis first passes the original input data into a deep network consisting of fully connected layers. Deep neural networks can handle non-linear functions that permit more complex features from the actual feature space. SFA is applied to the new complex feature space to attain a projecting matrix. It is then used to extract the most invariant parts of the HSI, facilitating the different pixels to be emphasized and finding the eigenvalues of the projecting matrix. The higher eigenvalues correspond to the most variant components in the HSI. Thresholding algorithms are used to generate the final change map.

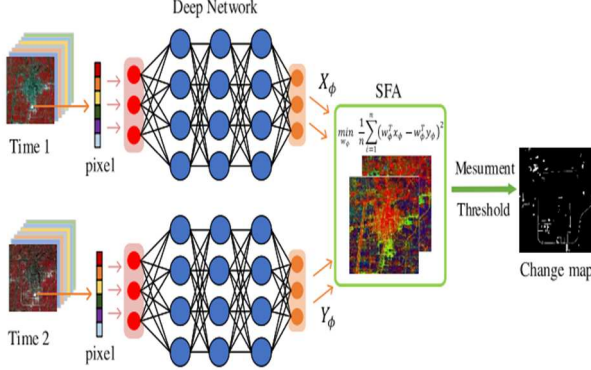


Fig. 2. Deep Slow Feature Analysis Architecture

DSFA consists of two portions. First one is the deep network module and the second is the SFA constraint. A deep network module consists of two fully connected symmetric networks use for the projection of the input into a new complex high-dimensional feature space.

The transformed features are given to SFA resulting in a projecting matrix, which extracts invariant components of multi-temporal hyperspectral images. From this the change pixels could be accentuated.

Change Vector Analysis is used to obtain the difference map, and K-means is used as a thresholding algorithm to obtain the binary change map. A gradient-based loss function is used to optimize the deep neural network parameters to increase its performance.

A. Formulation

Let's assume two remote sensing images $X, Y \in \mathbb{R}^{m \times n}$, where the feature band and pixels are represented by m and n respectively. Specified an example X , the yield of the first hidden layer could be formulated as

$$f_1^1(X) = s(w_1^1 X + b_1^1) \quad (3)$$

where $w_1^1 \in \mathbb{R}^{h_1 \times m}$ and $b_1^1 \in \mathbb{R}^{h_1}$ represent the weight matrix and bias vector, respectively, whereas $s(\cdot)$ is the activation function. And the output for all other hidden layers are calculated in the same way. But the output forth last hidden layer is $f_l^1(X) = s(w_l^1 f_{l-1}^1(X) + b_l^1)$, where $w_l^1 \in \mathbb{R}^{h_l \times h_{l-1}}$ and $b_l^1 \in \mathbb{R}^{h_l}$. After that it will be mapped by the output layer. Therefore the changed future of this network is

$$X_\phi = f(\phi_1, X) = s(w_0^1 f_l^1(X) + b_0^1) \quad (4)$$

where $w_0^1 \in \mathbb{R}^{0 \times h_1}$ and $b_0^1 \in \mathbb{R}^0$ are the weight and the bias vector, respectively and ϕ_1 represents the set of all network parameters. For instance Y , Y_ϕ has a symmetric expression

$$Y_\phi = f(\phi_2, Y) = s(w_0^2 f_l^2(X) + b_0^2) \quad (5)$$

When we get the high-dimensional feature space is mapped from the original data by the deep networks, let $X_\phi - \left(\frac{1}{n}\right) 1X_\phi$ and $\hat{Y}_\phi = Y_\phi - \left(\frac{1}{n}\right) 1Y_\phi$ denote the centralized X_ϕ and Y_ϕ , respectively. The calculation of the covariance matrix of transformed data:

$$\Sigma XX = \widehat{X}_\phi \widehat{X}_\phi^T + r \times I \quad (6)$$

$$\Sigma YY = \widehat{Y}_\phi \widehat{Y}_\phi^T + r \times I \quad (7)$$

$$\Sigma XY = (\widehat{X}_\phi - \widehat{Y}_\phi)(\widehat{X}_\phi - \widehat{Y}_\phi)^T \quad (8)$$

Let identity matrix be denoted by I and regularization constant be denoted by r , for this reason Σxx and Σyy will be positive, definite and invertible. Now to solve the generalized eigenvalue problem is formulated as:

$$A_\phi W = B_\phi W \Lambda \Leftrightarrow B_\phi^{-1} A_\phi W = W \Lambda \quad (9)$$

where $A_\phi = \Sigma XY$ and $B_\phi = (1/2)(\Sigma xx + \Sigma yy)$. According to (1-3), the final form the problem is

$$\left[\frac{1}{2} (\Sigma xx + \Sigma yy) \right]^{-1} \Sigma XY W = W \Lambda \quad (10)$$

According to the SH=FA theory, the best invariant element has the least eigenvalue. So the goal of the DSFA is to minimize the sum of the squares of all Eigen values so that the change pixel can be easily detected.

V. DATASETS

In this study, Indian Pines dataset is considered. This dataset covers the Purdue University and the surrounding area on 12th June, 1992 from the AVIRIS Hyperspectral sensor. Input image contains hyperspectral bands with 145x145 pixels. It represents different portions of electromagnetic spectrum with each pixel consisting of 220 spectral reflectance bands in the wavelength range 0.4–2.5 μ m. All the datasets were in the .mat format (matrix file).

VI. RESULTS AND DISCUSSIONS

To assess the performance of DSFA, we adopted TensorFlow and ran tests on a hyperspectral remote sensing image data set named the River data set, which was taken from Taizhou, Jiangsu, China. The size of this image is 400x400.

A. Description of Modules

- `Utils.py()` - Contains logic for Slow Feature Analysis and CVA used in change detection.
- `model.py()` - Contains a fully connected neural network before performing SFA.
- `createImageCubes()` - Contains logic to divide the given Hyperspectral image into patches of desired size. It is used before sending data to CNN for classification.
- `applyPCA()` - Applies PCA for dimensionality reduction for classification.



Fig. 3. Gray-scale images (a) 2002 and (b) 2003



Fig. 4. Ground-truth image of the changed and unchanged regions of Taizhou

Fig. 3 shows the images acquired of the region Taizhou. Fig. 3 (a) is acquired in 2002, and fig. 3 (b) is acquired in 2003 of the same location. Fig. 4 shows the changes in the duration from 2002 to 2003 of the region Taizhou. It represents the changed region versus the unchanged region, where the white pixels represent the changed regions and black pixels represent the unchanged regions. The changed region comprises 4,227 pixels, and the unchanged region comprises 17,163 pixels.

The experimentation on the Taizhou dataset with 4000 pixels which account for about 2.5% of the total number of pixels was carried with DSFA. These pixels are randomly selected from the unchanged area of CVA for training; this is done to fetch the network parameters and the SFA projecting matrix.

To evaluate the HSI change detection performance, we have used Overall Accuracy (OA) as the evaluation metric, as it denotes the number of actually changed pixels in the samples out of the total test samples.

TABLE I. DSFA CHANGE DETECTION

Method	Device	Time taken (in seconds)	Overall Accuracy (in %)
DSFA	Personal Computer(PC)	21.14	88.40
DSFA	NVidia DGX-1	13.40	90.27

We ran the change detection algorithm on a personal computer (spec- 8GB RAM, Intel core i57300HQ, cup @ 2.5 GHz) without CUDA and also on the DGX-1 server (8 GPU's each of 32 GB RAM), which took approximately 21.14 seconds and obtained an accuracy of 88.40% and 13.40 seconds with 90.27% accuracy respectively.

And for classification, we used Indian Pines (IP) and Salinas Scene (SA) HSI data sets publicly available. The Indian Pines dataset has images with spatial dimension 145 x 145, and the wavelength ranged from 400 to 2500 nm with 224 spectral bands, out of which 24 spectral bands have been discarded as they covered the region of water absorption. Sixteen classes of vegetation have been designated as ground truth.

TABLE II. HYBRIDSN CLASSIFICATION

Method	Device	Time taken (in seconds)	Overall Accuracy (in %)
Hybrid SN	Personal Computer(PC)	98.14	98.40
Hybrid SN	NVidia DGX-1	8.12	99.75

The Salinas Scene dataset has images with spatial dimension 512x217 with wavelength ranging from 360-2500 nm. It had 224 spectral bands, out of which 20 water-absorbing spectral bands have been thrown away. This dataset also has 16 classes as ground truth.



Fig. 5. Input Image



Fig. 6. Target Image (window size 37)



Fig. 7. Target Image (window size 25)



Fig. 8. Target Image (window size 17)



Fig. 9. Target Image (window size 9)



Fig. 10. Classes

The input image Fig. 5 is pre-processed and then passed to the neural network, which gives the target image Fig. 6 as output with the classes mentioned in Fig. 10.

We ran the classification algorithm in our personal computer (spec- 8GB RAM, Intel core i57300HQ, cup @ 2.5Ghz,) without CUDA and also in the DGX-1 server (8 GPU's each of 32 GB RAM), which took approximately 98.14 seconds and obtained an accuracy of 98.40% and 8.14 seconds with 99.75% accuracy respectively.

To judge the HSI classification performance, we used Overall Accuracy (OA) as the evaluation metric, as it characterizes the number of adequately classified samples out of the total test samples.

TABLE III. OVERALL ACCURACY (OA) OF DATASETS WITH VARYING WINDOW SIZE

Window Size	Salinas Scene (OA)	Indian Pines(OA)
9 x 9	99.79	99.73
17 x 17	99.86	99.54
25 x 25	100	99.75
37 x 37	99.98	99.71

From the Table III, we can infer that we obtain good accuracy if the window size is big, but not in all cases as 9x9 gave good accuracy than 37x37 in the Indian Pines data set. So we can say that it differs from one data set to another.

Other factors like the number of epoch and learning rate also contribute to the resulting accuracy but increasing the number of epochs is not that significant; more important is the validation and training error.

As long as these two errors keep drooping, training should continue. Usually, the number of epoch depends on the batch size. Regularization needs to be done to counter overfitting in order to get good accuracy.

VII. CONCLUSION

To identify the changes, we used a Hybrid Spectral Net classification algorithm for the HSI data set with ground-truth and the DSFA, a change detection method for hyperspectral images. As mentioned earlier, we aimed to combine both the algorithms and perform multi-class classification for a common data set having both ground-truth and bi-temporal images. But the dataset availability is limited, so we used different data sets to perform change detection and classification. We combined 2D convolution and 3D

convolution layers to form a hybrid that performs better than conventional 2D or 3D convolutions in classification.

In DSFA, the SFA extracts the best invariant components of the unchanged pixels. It subdues them to focus on the changed components. This method is used to differentiate the changed versus unchanged components in a bi-temporal image. If a common data set is to be found then, multi-class change detection would be possible from which we could highlight which regions of a particular class is changed over a period of time, which would help in military surveillance to prevent enemy invasions in advance and also in the medical field to detect changes in the organs to draw relevant conclusions required for the proper treatment. There are many more fields where multi-class classification could prove useful.

ACKNOWLEDGMENT

We extend our gratitude to KLE Technological University for the endowment in undertaking research.

REFERENCES

- [1] Jianya, Gong, Sui Haigang, Ma Guorui, and Zhou Qiming. "A review of multi-temporal remote sensing data change detection algorithms." *The International Archives of the Photogrammetry, Remote Sensing and Spatial Information Sciences* 37, no. B7 (2008): 757-762.
- [2] Song, Ahram, Jaewan Choi, Youkyung Han, and Yongil Kim. "Change detection in hyperspectral images using recurrent 3D fully convolutional networks." *Remote Sensing* 10, no. 11 (2018): 1827.
- [3] Kwan, Chiman. "Methods and challenges using multispectral and Hyperspectral images for practical change detection applications." *Information* 10, no. 11 (2019): 353.
- [4] Khelifi, Lazhar, and Max Mignotte. "Deep learning for change detection in remote sensing images: Comprehensive review and meta-analysis." *IEEE Access* 8 (2020): 126385-126400.
- [5] Du, Bo, Lixiang Ru, Chen Wu, and Liangpei Zhang. "Unsupervised deep slow feature analysis for change detection in multi-temporal remote sensing images." *IEEE Transactions on Geoscience and Remote Sensing* 57, no. 12 (2019): 9976-9992.
- [6] Roy, Swalpa Kumar, Gopal Krishna, Shiv Ram Dubey, and Bidyut B. Chaudhuri. "HybridSN: Exploring 3-D-2-D CNN feature hierarchy for hyperspectral image classification." *IEEE Geoscience and Remote Sensing Letters* 17, no. 2 (2019): 277-281.
- [7] López-Fandiño, Javier, Alberto S. Garea, Dora B. Heras, and Francisco Argüello. "Stacked autoencoders for multiclass change detection in hyperspectral images." In *IGARSS 2018-2018 IEEE International Geoscience and Remote Sensing Symposium*, pp. 1906-1909. IEEE, 2018.
- [8] Bidari, Indira, Satyadhyam Chickerur, Harivijay Ranmale, Sushmita Talawar, Harish Ramadurg, and Rekha Talikoti. "Hyperspectral Imagery Classification Using Deep Learning." In *2020 Fourth World Conference on Smart Trends in Systems, Security and Sustainability (WorldS4)*, pp. 672-676. IEEE, 2020.
- [9] Ghamisi, Pedram, Naoto Yokoya, Jun Li, Wenzhi Liao, Sicong Liu, Javier Plaza, Behnood Rasti, and Antonio Plaza. "Advances in hyperspectral image and signal processing: A comprehensive overview of the state of the art." *IEEE Geoscience and Remote Sensing Magazine* 5, no. 4 (2017): 37-78.
- [10] Bidari, Indira, Satyadhyam Chickerur, Rekha M. Talikoti, Smita S. Kapali, Sushmita Talawar, and Soumya Sangam. "Performance Analysis of Change Detection Algorithms on Multispectral Imagery." In *2020 12th International Conference on Computational Intelligence and Communication Networks (CICN)*, pp. 81-86. IEEE, 2020.
- [11] Hasanlou, Mahdi, and Seyd Teymoor Seydi. "Hyperspectral change detection: An experimental comparative study." *International journal of remote sensing* 39, no. 20 (2018): 7029-7083.